

CN Andromedae: a shallow contact binary with a possible tertiary component

Muhammed Faruk Yildirim, Fahri Aliçavuş and Faruk Soyduğan

Çanakkale Onsekiz Mart University, Faculty of Arts and Sciences, Department of Physics, 17020, Çanakkale, Turkey;
fsoydugan@comu.edu.tr

Çanakkale Onsekiz Mart University, Astrophysics Research Center and Ulupınar Observatory, 17020, Çanakkale, Turkey

Received 2018 June 19; accepted 2018 July 30

Abstract In this study, new photometric observations of shallow contact binary CN Andromedae (CN And) were performed and multi-color (BVR) CCD light curves (LCs) were obtained. Simultaneous analysis of new LCs and published radial velocity (RV) data reveals that the system is an early contact binary in which both components have recently filled their inner Roche lobes. Asymmetric LCs were modeled by a dark spot on the primary component and a hot spot on the secondary component that probably resulted from magnetic activity and mass transfer, respectively. Modeling of LCs and RV data allows us to estimate the following absolute parameters: $M_1 = 1.40 \pm 0.02 M_\odot$, $M_2 = 0.55 \pm 0.01 M_\odot$, $R_1 = 1.45 \pm 0.02 R_\odot$ and $R_2 = 0.94 \pm 0.02 R_\odot$. A decreasing orbital period with a rate of $dP/dt = -1.5 \times 10^{-7} \text{ d yr}^{-1}$ can be seen as evidence that the system is evolving into a contact binary with higher contact degree. Cyclic oscillation of the $O - C$ data was interpreted by the Applegate mechanism and light-time effect due to an unseen component around the close binary system. The hypothetical third component is probably a fully convective red dwarf star with a minimal mass of $0.1 M_\odot$. CN And is at the early phase of the contact stage of its evolution and is an interesting example for studying the formation and evolution of close binaries.

Key words: binaries: eclipsing — stars: fundamental parameters — stars: individual (CN And)

1 INTRODUCTION

Contact binaries are important sources for investigating the evolution of close binary stars and the process of mass loss and transfer, angular momentum loss and tidal interactions. They are also known as W UMa type eclipsing binaries, according to the shape of their light curves. The orbital periods of these systems are generally between 0.2–1 d and mass ratios of the components are mostly between 0.1 and 0.5. The eclipse depths in the light curves of most contact binaries are usually equal since both components have nearly the same surface temperature although their masses may be different due to several factors. Evolutionary status around the contact phase can be generally explained by thermal relaxation oscillation (TRO) theory (Lucy 1967a; Flannery 1976; Robertson & Eggleton 1977). W UMa binaries around the contact phase, known as early or shallow contact binaries, have components with different temperatures; therefore, different eclipse depths for the primary and secondary minima in their light curves are seen. This

type of close binary is also essential for studying the initial stages of the contact phase since the evolutionary stage contains many unknowns.

CN Andromedae (CN And, TYC 2787-1815-1, GSC 02787-01815) was discovered by Hoffmeister (1949), who firstly announced that the system shows β Lyr-type light variations. Tsesevich (1956) reported that the system is an Algol type binary with an orbital period of 2.599 d. It was stated by Löchal (1960) that CN And has a W UMa type light curve and its orbital period is 0.462798 d. Bozkurt et al. (1976) revealed asymmetric changes in the B and V light curves. Kaluzny (1983) reported that the light curves of the system showed β Lyr-type variations due to the two minima clearly having different depths. Two flares were observed in the light curve of the system obtained in 1981 by Yang & Liu (1985). Shaw et al. (1996) reported strong X-ray emission for the system. Photometric observations of CN And have been carried out by several authors (e.g. Bozkurt et al. 1976; Kaluzny 1983; Michaels et al. 1984; Evren et al. 1987; Samec et al. 1998; Van Hamme et al.

2001; Zola et al. 2005; Lee & Lee 2006; Koju & Beaky 2015).

Light curve analysis of the system was made by Van Hamme et al. (2001); Çiçek et al. (2005); Lee & Lee (2006). Additionally, the light curves in *BVRI* filters of CN And were presented and the O’Connell effect and period variation of the system discussed by Koju & Beaky (2015). Rucinski et al. (2000) published radial velocity measurements and obtained the spectroscopic orbital elements of the system. The spectral type of the components was suggested as being in the range of F5-G5 by Zola et al. (2005). Siwak et al. (2010) published the most recent radial velocity and light curve analysis of the system. Orbital period variations of CN And were investigated by several authors (e.g Kaluzny 1983; Evren et al. 1987; Samec et al. 1998; Van Hamme et al. 2001; Çiçek et al. 2005; Lee & Lee 2006). Lastly, Koju & Beaky (2015) studied the period changes of the system and the decreasing orbital period was explained by mass transfer from the primary component to the secondary one with a rate of $4.82(6) \times 10^{-8} M_{\odot} \text{yr}^{-1}$.

2 OBSERVATIONS

New CCD observations of CN And were made at Çanakkale Onsekiz Mart University (ÇOMÜ), Ulupınar Astrophysics Observatory during the 2013 (three nights) and 2017 (eight nights) observing seasons. The observations were performed using a 30-cm LX200 model Schmidt-Cassegrain reflector equipped with an ALTA U47 CCD camera (Peltier cooling, E2V CCD47-10 chip, 1024×1024 pixels, $13 \times 13 \mu\text{m}$ pixel size). This CCD camera provides an observed field of view of $15 \text{ arcmin} \times 15 \text{ arcmin}$. All observations were made with the *BVR* filters. TYC 2786 406 and TYC 2787 1843 were used as comparison and check stars, respectively. During the observations, no significant light variation for the comparison or check stars was found. Exposure times were selected to be 10, 4 and 3 seconds for *B*, *V* and *R* filters, respectively. The CCD data were reduced following standard reduction procedures: bias and dark frames were subtracted from the science frames and then corrected for flat fielding. The reduced CCD images were used to calculate the differential magnitudes. For the reduction process, the C-Munipack program written by D. Motl (2007; <http://c-munipack.sourceforge.net>) was used. Observational errors measuring the magnitudes in all filters were calculated as approximately 0.01^{m} . In addition to the *BVR* light curves as seen in Figure 1, four primary and seven secondary minima times were obtained during the observations.

3 SIMULTANEOUS ANALYSIS OF LIGHT AND RADIAL VELOCITY CURVES

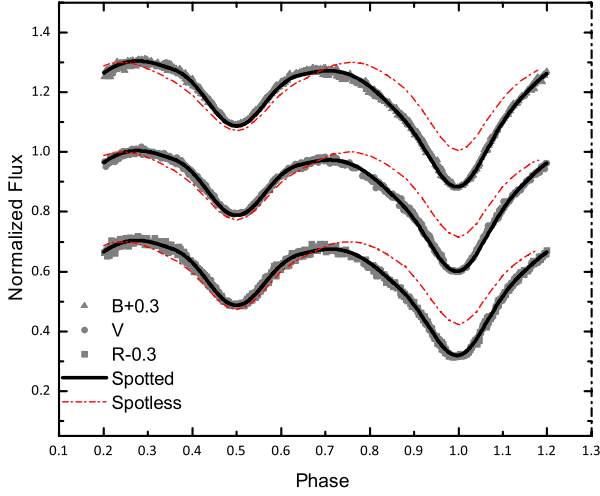
In order to analyze the *BVR* light curves obtained in this work and the radial velocity curves taken from Rucinski et al. (2000), we used the 2003 version (van Hamme & Wilson 2003) of the Wilson-Devinney (WD) code (Wilson & Devinney 1971). The WD method requires that the input parameters are reasonable, as any method applied for light curve analysis of eclipsing binaries. In addition, some parameters should be fixed; therefore they should be estimated from convenient theoretical models. The adopted parameters were as follows: the temperature of the primary component was taken as 6350 K from Cox (2000) based on its spectral type F6V, which was estimated from the $(B - V) = 0.47 \text{ mag}$ value of the system given in the APASS Catalog¹. The logarithmic limb darkening coefficients were taken from van Hamme (1993), while the bolometric gravity-darkening coefficient $g_{1,2}$ was set to 0.32 for convective envelopes (Lucy 1967b). The bolometric albedos $A_{1,2}$ were fixed to 0.5 for convective envelopes from Ruciński (1969). Synchronous rotation for the primary and secondary components ($F_1 = F_2 = 1$) and circular orbit ($e = 0$) were accepted before analysis. The adjustable parameters were light elements (reference epoch T_0 and period P) together with the length of the semi-major axis of the relative orbit (a), radial velocity of the binary system’s center of mass (V_{γ}), orbital inclination to the plane of the sky (i), flux-weighted average surface temperature of the secondary component (T_2), mass ratio ($q = m_2/m_1$), non-dimensional normalized surface potentials of the components ($\Omega_{1,2}$) and the fractional monochromatic luminosity of the primary component (L_1).

At the beginning of the analysis, the mass ratio of $q = 0.39$ obtained spectroscopically by Rucinski et al. (2000) was chosen as a starting input value. In order to model the asymmetric light curves as seen in Figure 1 and Table 1, a dark spot on the primary component and a hot spot on the secondary one were considered, as applied by Lee & Lee (2006); Çiçek et al. (2005); Van Hamme et al. (2001). The dark spot can be explained by magnetic activity on the surface of the primary component, while mass transfer from the more massive component to the less massive one may result in a hot spot on the secondary component. Analysis began in detached mode and then continued in contact mode (Mode 3 in the WD code) since the critical surface potentials of the components had reached their

¹ APASS Catalog: The AAVSO Photometric All-Sky Survey, <https://www.aavso.org/apass>

Table 1 Light levels at 0.25 and 0.75 orbital phases and their differences in light curves of CN And.

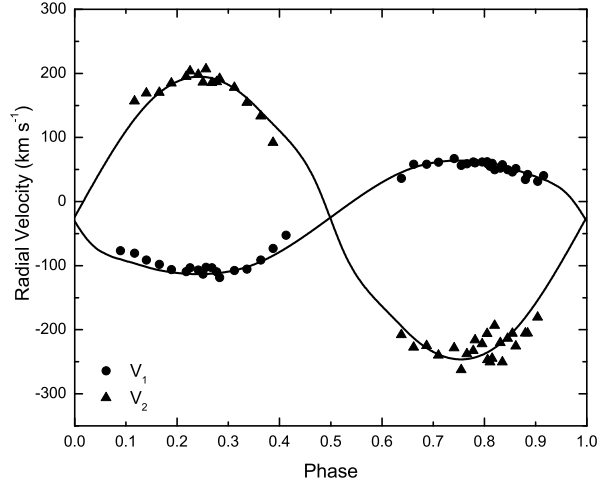
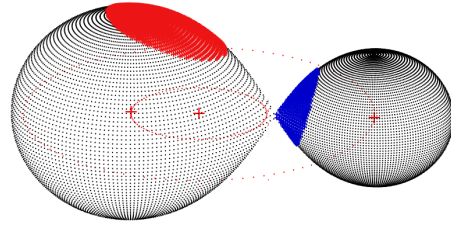
| | <i>B</i> | <i>V</i> | <i>R</i> |
|---------------------------------|-----------|-----------|-----------|
| 0.75 (Max. Light) | −1.032(5) | −0.531(4) | −0.185(5) |
| 0.25 (Max. Light) | −1.081(4) | −0.577(4) | −0.232(3) |
| $\Delta m(m_{0.75} - m_{0.25})$ | 0.049 | 0.045 | 0.047 |
| $(\Delta m) \times 1000$ | 49(9) | 45(8) | 47(8) |


Fig. 1 Observational points of CN And with theoretical light curves corresponding to parameters obtained from the simultaneous solution of *BVR* light and radial velocity curves. Continuous black lines indicate the case of a dark spot and a hot spot. The dash-dotted red lines signify the case without spots.

limiting values. Although the third light was set as a free parameter, we could not find a meaningful third light contribution and therefore it was negligible during the analysis. Combining our photometric data with the radial velocities of components given by Rucinski et al. (2000), a simultaneous analysis of light and radial velocity curves was obtained. The results are given in Table 2 together with previous studies. A comparison of theoretical fits and observational data for the light and radial velocity curves can be seen in Figures 1 and 2, respectively. Geometric configuration at orbital phase 0.25 with the dark and hot spots is illustrated in Figure 3.

4 LONG-TERM ORBITAL PERIOD CHANGES

The orbital period of CN And is changing, as revealed in several studies based on eclipse times (e.g. Çiçek et al. 2005; Lee & Lee 2006). All published results on the analysis of *O – C* data indicate that its period is decreasing. In order to update the orbital period analysis and to uncover any possible changes, we collected all published minima times (CCD, photoelectric and visual) from the literature


Fig. 2 Observational and theoretical radial velocity curves of CN And. Filled circles represent the primary component and triangles indicate the secondary component.

Fig. 3 Geometrical structure of components of CN And at orbital phase 0.25.

and the new times of four primary (I) and seven secondary minima (II) were obtained during observations. Observed eclipse times of minima and their errors, which were determined by using the method of Kwee & van Woerden (1956), are given in Table 3. These minima times are given as averaged values of the eclipse times obtained in *BVR* colors during the same night. In order to analyze variations in the orbital period of the system, we used the *O – C* method, as applied in many studies (e.g. Soyduğan 2008; Yang et al. 2010). In the *O – C* diagrams of CN And, the orbital period changes can be seen clearly. We discovered a periodic signal in the *O – C* data in addition to a downward parabola, as noted in all previous studies on the orbital period variations. Therefore, both parabolic and periodic variations were considered for analysis.

As demonstrated in Figure 4, the general trend of *O – C* data can be represented by a downward parabola indicating an orbital period decrease. In this case, the following equation is used to model the *O – C* data

$$\begin{aligned} \text{HJD (MinI)} = & 2458000.3841(5) \\ & + 0.46278940(4)^d \times E \\ & - 9.60(4) \times 10^{-11} \times E^2. \end{aligned} \quad (1)$$

Table 2 Result of analyses of simultaneous light and radial velocity curves obtained by the WD method.

| Parameter | van Hamme et al. (2001, <i>UBV</i>) | Çiçek et al. (2005, <i>BVR</i>) | Lee & Lee (2006, <i>BVRI</i>) | Siwak et al. (2010, <i>BVRI</i>) | This Study (<i>BVR</i>) |
|-----------------------------------|---|-------------------------------------|-----------------------------------|--------------------------------------|------------------------------|
| T_0 (HJD+2400000) | 50698.9430(1) | 52185.4226(1) | 46711.5318(8) | 52500.1204 | 58000.3841(5) |
| P (d) | 0.4627952(35) | 0.46278845(3) | 0.46279252(1) | 0.46279081 | 0.46278940(4) |
| i ($^\circ$) | 68.51 (17) | 68.02 (15) | 69.9 (1) | 69.416(92) | 67.802 (145) |
| T_1 (K) | 6500 | 6500 | 6500 | 6450 | 6350 |
| T_2 (K) | 5922 (24) | 5947 (12) | 5890 (4) | 4726(34) | 5732 (35) |
| $\Omega_1 = \Omega_2$ | 2.654 (4) | 2.667 (6) | 2.658 (2) | 2.6403(12) | 2.651 (3) |
| q | 0.3885 (22) | 0.3935 (20) | 0.390 (1) | 0.385(5) | 0.387 (4) |
| a (R_\odot) | 3.066 (3)5 | 3.16 (2) | 3.00 (1) | 3.163(22) | 3.14 (1) |
| V_γ (km s^{-1}) | -24.2 (1) | -25.89 (66) | -22.3 (9) | -23.47(63) | -25.5 (4) |
| $A_1 = A_2$ | 0.5 | 0.5 | 0.5 | 0.5 | 0.5 |
| $g_1 = g_2$ | 0.32 | 0.32 | 0.32 | 0.32 | 0.32 |
| $L_1/(L_1 + L_2)_B$ | 0.8087 (61) | 0.7982 (26) | 0.8140 (29) | 0.927(2) | 0.808 (4) |
| $L_1/(L_1 + L_2)_V$ | 0.7858 (56) | 0.7782 (26) | 0.7890 (25) | 0.912(2) | 0.796 (5) |
| $L_1/(L_1 + L_2)_R$ | – | 0.7649 (22) | 0.7737 (23) | 0.897(1) | 0.782 (5) |
| $L_1/(L_1 + L_2)_I$ | – | – | 0.7618(21) | 0.827(1) | – |
| $L_2/(L_1 + L_2)_B$ | 0.191 | 0.2018 | 0.1860 | 0.073(3) | 0.192 |
| $L_2/(L_1 + L_2)_V$ | 0.214 | 0.2222 | 0.2110 | 0.088(4) | 0.204 |
| $L_2/(L_1 + L_2)_R$ | – | 0.2351 | 0.2263 | 0.103(4) | 0.218 |
| $L_2/(L_1 + L_2)_I$ | – | – | 0.2382 | 0.127(4) | – |
| r_1 (pole) | 0.435 (1) | – | – | – | 0.4347 (2) |
| r_1 (side) | 0.465 (1) | – | – | – | 0.4642 (3) |
| r_1 (back) | 0.491 (1) | – | – | – | 0.4909 (3) |
| r_2 (pole) | 0.279 (1) | – | – | – | 0.2806 (2) |
| r_2 (side) | 0.291 (2) | – | – | – | 0.2925 (2) |
| r_2 (back) | 0.323 (2) | – | – | – | 0.3252 (4) |
| Filling Rate | 99 | 99 | 99 | – | 100 |
| f (%) | – | – | – | 3 | 0 |
| Spot Parameter | | Primary Component | | | |
| θ ($^\circ$) | 22.3 (24) | 22.6 (45) | 19.8 (20) | – | 22(3) |
| ϕ ($^\circ$) | 16.9 (20) | 17.5 (35) | 11.5 (20) | – | 15(3) |
| r ($^\circ$) | 32.9 (20) | 32.1 (64) | 34.9 (10) | – | 35(1) |
| $T_f = T_s/T_*$ | 0.650 | 0.650 | 0.650 | – | 0.650 |
| Spot Parameter | | Secondary Component | | | |
| θ ($^\circ$) | 84 (5) | 83.1 (2) | 87.5 (20) | 90 | 80(2) |
| ϕ ($^\circ$) | 1.1 (20) | 1.3 (3) | 3.6 (23) | 11.49(36) | 1(2) |
| r ($^\circ$) | 19.5 (18) | 20.1 (4) | 23.30 (21) | 113.9(19) | 30(4) |
| $T_f = T_s/T_*$ | 1.104 (13) | 1.093 (22) | 1.092 (14) | 1.2138(72) | 1.100(20) |

In Figure 4, the parabolic fit to the $O - C$ data can be seen. The quadratic term of $Q = -9.60 \times 10^{-11}$ d leads to a continuous period decrease rate of $dP/dt = -3.3 \times 10^{-7}$ d yr $^{-1} = 1.31$ s century $^{-1}$. The residuals from the parabolic representation indicate clear cyclic variations. Therefore, we used two different mechanisms to explain the periodic behavior of the orbital period of the system.

4.1 Third Body

Unseen components physically connected in a binary system produce periodic changes in the $O - C$ diagrams. In

this study, taking into account the distribution of $O - C$ data of CN And, we used the following formula to calculate minima times

$$\begin{aligned} \text{HJD (MinI)} = & 2458000.3841(5) \\ & + 0.46278940(4)^d \times E \quad (2) \\ & - 9.60(4) \times 10^{-11} \times E^2 + \Delta t . \end{aligned}$$

In this equation, the first three terms on the right were obtained from the parabolic representation. Δt is the time delay that resulted from the third component in the close binary system. The basic expression for modeling periodic variations in $O - C$ diagrams resulting from the light-time

Table 3 New Minima Times of CN And

| Filters | Minima Times (HJD+2400000) | Errors | Type (I/II) |
|----------------|-------------------------------|--------|----------------|
| <i>V, R</i> | 56468.5473 | 0.0001 | I |
| <i>B, V, R</i> | 56528.4799 | 0.0003 | II |
| <i>V, R, I</i> | 56555.3202 | 0.0003 | II |
| <i>B, V, R</i> | 57977.4765 | 0.0003 | II |
| <i>B, V, R</i> | 57990.4353 | 0.0002 | II |
| <i>B, V, R</i> | 58000.3830 | 0.0002 | I |
| <i>B, V, R</i> | 58000.3841 | 0.0001 | I |
| <i>B, V, R</i> | 58009.4085 | 0.0003 | II |
| <i>B, V, R</i> | 58013.3405 | 0.0002 | I |
| <i>B, V, R</i> | 58035.3227 | 0.0002 | II |
| <i>B, V, R</i> | 58041.3402 | 0.0001 | II |

Table 4 Parameters and their errors from $O - C$ analysis based on LITE and quadratic representation for CN And.

| Parameter | Value |
|------------------------|----------------------------|
| T_0 (HJD+2400000) | 58000.3841(5) |
| P_{orb} (d) | 0.46278940(4) |
| Q (d) | $-9.60(4) \times 10^{-11}$ |
| $a_{12} \sin i$ (AU) | 0.72(5) |
| e | 0 ^a |
| ω (°) | 90 ^a |
| T' (HJD+2400000) | 54579(658) |
| P_{12} (yr) | 38(4) |
| $f(m_3)$ (M_\odot) | 0.00025(5) |
| m_3 (M_\odot) | |
| ($i = 90^\circ$ for) | 0.10 |

Notes: ^a Adopted.

effect (LITE) was first given by Irwin (1959)

$$\Delta t = \frac{a_{12} \sin i'}{c} \times \left\{ \frac{1 - e'^2}{1 + e' \cos \nu'} \sin(\nu' + \omega') + e' \cos \omega' \right\}, \quad (3)$$

where a_{12} , i' , e' , ν' and ω' are the semi-major axis, inclination, eccentricity, true anomaly of the position of the binary system's mass center of orbit and the longitude of the periastron of the orbit of the eclipsing binary around the third component, respectively. The resulting parameters found from $O - C$ analysis are listed in Table 4. The parabolic and LITE representations are seen together with the $O - C$ data in Figure 4, while only the LITE fit is indicated in Figure 5.

4.2 Applegate Model

In binary stars, when at least one of the components has a convective outer envelope, magnetic activity may be expected. In this case, the orbital period of these active systems may indicate cyclic orbital period variations, as discussed for several systems (e.g Qian et al. 2004; Zhang

Table 5 Applegate Parameters of CN And

| Parameter | Value |
|---------------------------------------|-----------------------|
| P_{mod} (yr) | 37 |
| $\Delta P/P$ | 1.95×10^{-6} |
| ΔJ (erg s ⁻¹) | 1.0×10^{47} |
| $\Delta \Omega/\Omega$ | 0.0003 |
| ΔE (erg) | 1.1×10^{40} |
| I_s (g cm ²) | 1.9×10^{54} |
| ΔL_{rms} (L_\odot) | 0.007 |
| B (kG) | 4.0 |

et al. 2014). Applegate (1992) proposed a model to interpret cyclic orbital period changes in binary stars that showed magnetic activity. According to this model, the $O - C$ variations of CN And resulted from a magnetic cycle that can be seen in cyclic form and are represented by the following equation

$$\begin{aligned} \text{HJD (MinI)} = & 2458000.3841(5) \\ & + 0.4678940(4)^d \times E \\ & + -9.60(4) \times 10^{-11} \times E^2 \\ & + A_{\text{mod}} \sin \left[\frac{2\pi}{P_{\text{mod}}} (E - T_s) \right], \end{aligned} \quad (4)$$

where A_{mod} , P_{mod} and T_s are the semi-amplitude, period of sinusoidal changes and time of minimum of sinusoidal variation, respectively. Values of linear and quadratic terms were used as calculated in the previous section since we could not find a meaningful variation during the analysis. In this model, we assumed that cyclic variations of the orbital period resulted from magnetic activity of the primary component. The equation was applied to the $O - C$ data using the regression method and the parameters of the sinusoidal variation were obtained with their errors. The resulting parameters ($P_{\text{mod}} = 37 \pm 4$ yr and $A_{\text{mod}} = 0.0042 \pm 0.0004$ d) were used to calculate the model parameters defined by Applegate (1992), which are listed in Table 5. Application of the model for various eclipsing binaries and explanations of the Applegate parameters are given in various studies (e.g. Soydugan 2008; Khaliullina 2017).

5 RESULTS AND DISCUSSION

From the photometric solution based on new CCD light curves, CN And is a shallow contact binary system with a mass ratio of $q = 0.387 \pm 0.004$. The system can also be classified as a near-contact binary according to the study of Zhu & Qian (2009) since both components are in marginal contact and have different surface temperatures ($\Delta T \approx 620$ K). The results indicate that the system is probably at the early contact phase. In order to study the

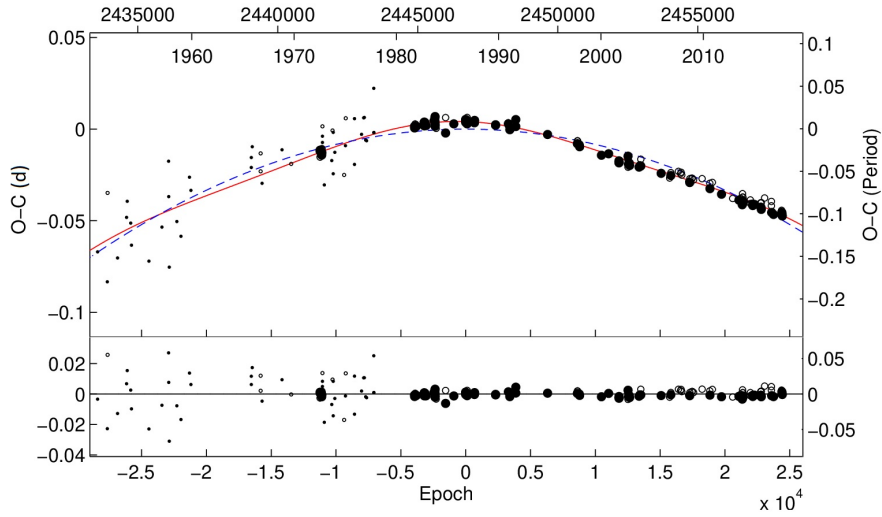


Fig. 4 Upper panel: Distribution of $O - C$ data, parabolic (dashed line) and parabolic plus cyclic representation (solid line) for CN And. Bottom panel: Residuals from best fit.

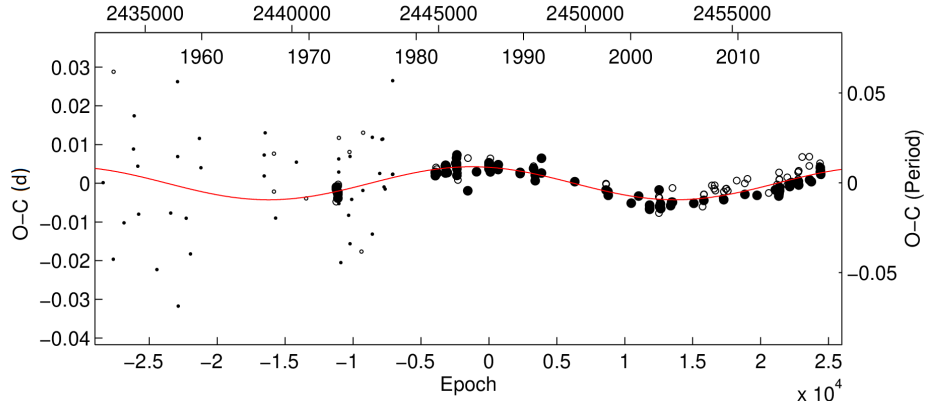


Fig. 5 Periodic variation of $O - C$ data for CN And with its theoretical representation calculated using LITE (continuous line).

transition process from the near-contact or early contact phase to deeper contact phase, CN And is a noteworthy example since the inner Roche lobes of the components have only recently been filled. Multi-color light curves of the system have asymmetries, as noted in previous studies, probably due to magnetic activity of the massive component and mass and/or energy transfer from the primary to the secondary companion (see Tables 1 and 2). The complex nature of the asymmetric behavior was modeled with a hot spot on the secondary and a dark spot on the primary component, which may be explained by the same astrophysical processes. The combined solution of the radial velocity data of the components and new CCD light curves allowed us to calculate the absolute parameters of the components and the orbital properties of the system. Solar values ($T_{\text{eff},\odot} = 5777 \text{ K}$, $M_{\text{bol},\odot} = 4.74 \text{ mag}$) and also bolometric corrections of the components are from Drilling &

Landolt (2000). The resulting basic astrophysical parameters are listed in Table 6 and agree well with previous studies by Çiçek et al. (2005); Siwak et al. (2010). The photometric distance of the system was found to be comparable with *Gaia* Data Release 2 (DR2) results within 2σ (Gaia Collaboration et al. 2016, 2018).

In order to compare several marginal contact binaries and also review their evolutionary status, we plotted their components on the plane of $\log T_{\text{eff}} - \log L$ (see Fig. 6). The components of four weak contact binaries: CN And (this study), PY Vir (Zhu et al. 2013), BX And (Yakut & Eggleton 2005) and TT Cet (Deb & Singh 2011), can be seen in Figure 6. Evolutionary tracks, and ZAMS and TAMS lines were formed based on MIST models for single stars and solar chemical composition (Paxton et al. 2011, 2013, 2015; Dotter 2016; Choi et al. 2016). As shown in Figure 6, the primary component of CN And is located in

Table 6 Basic astrophysical parameters and their probable errors for CN And

| Parameter | van Hamme et al. (2001) | Çiçek et. al. (2005) | Siwak et. al. (2010) | This Study |
|--------------------------|-------------------------|----------------------|----------------------|------------|
| $M_1 (M_\odot)$ | 1.30(5) | 1.42(3) | 1.433(30) | 1.40(2) |
| $M_2 (M_\odot)$ | 0.51(2) | 0.56(2) | 0.552(20) | 0.55(1) |
| $R_1 (R_\odot)$ | 1.43(2) | 1.48(1) | 1.48(3) | 1.45(2) |
| $R_2 (R_\odot)$ | 0.92(1) | 0.94(1) | 0.95 | 0.94(2) |
| T_1 (K) | 6500 | 6500 | 6450 | 6350 (200) |
| T_2 (K) | 5922(24) | 5947(12) | 4726 | 5732 (200) |
| $\log g_1$ (cgs) | 4.24 | 4.25(1) | — | 4.26(1) |
| $\log g_2$ (cgs) | 4.22 | 4.24(1) | — | 4.23(2) |
| $M_{\text{bol},1}$ (mag) | 3.46 | 3.38(2) | — | 3.49(2) |
| $M_{\text{bol},2}$ (mag) | 4.83 | 4.75(4) | — | 4.91(4) |
| $L_1 (L_\odot)$ | — | 3.52(7) | 3.40 | 3.41(9) |
| $L_2 (L_\odot)$ | — | 0.998(34) | 0.40 | 0.93(4) |
| $E(B - V)$ | — | — | — | 0.07(1) |
| d (pc) | — | 210(15) | — | 181(13) |
| d_{Gaia} (pc) | — | — | — | 201(2) |

Table 7 Four Near-contact Binaries with Orbital Periods and Basic Parameters

| System | Period | Spectral Type | System Type | $O - C$ Variation Type | Reference |
|----------|-------------------------|----------------------|---------------------|---|-----------|
| BX And | 0.610112 ^[1] | F2V ^[2] | Contact binary | Downward Par.+Sinusoidal ^[1] | [1, 2] |
| TT Cet | 0.485954 ^[1] | F4V ^[3] | Contact binary | Downward Par. ^[1] | [1, 3] |
| RV Crv | 0.747250 ^[1] | F2/K5 ^[4] | Near-contact binary | Downward Par. ^[1] | [1, 4] |
| V361 Lyr | 0.309614 ^[1] | F8/K1 ^[5] | Near-contact binary | Downward Par. ^[1] | [1, 5] |

References: [1] Kreiner et al. (2001); [2] Siwak et al. (2010); [3] Duerbeck & Rucinski (2007); [4] Shaw et al. (1996); [5] Hilditch et al. (1997).

the middle of the main-sequence band, while the secondary component is close to the ZAMS line. A less massive component of CN And is overluminous and has a higher effective temperature. Its position on the $\log T_{\text{eff}} - \log L$ plot is not compatible with the evolutionary track according to its mass, as seen in many contact binaries. On the other hand, the secondary components of PY Vir and TT Cet are near the evolutionary tracks calculated by their masses, while the cooler component of BX And is more evolved among shallow contact binaries.

In view of the dynamical evolution of cool detached binaries into contact binaries, Eker et al. (2006) defined a border between detached and contact binaries on the plane of $\log J_0 - \log M$. Orbital angular momentum (J_0) and total mass (M) of the system give an important clue about the dynamical evolution of detached binaries with cool components. Orbital angular momentum loss causes detached systems to turn into contact binaries. The contact border investigated by Eker et al. (2006) also provides a means of checking the Roche configurations of the near-contact and shallow contact binaries. CN And is seen in the early contact phase and both components have recently filled their inner Roche lobes, based on the simultaneous

light and radial velocity curves. It can be seen that the system is located in the contact region, near the contact border on $\log J_0 - \log M$ (see Fig. 4 given by Eker et al. 2006), which supports our results obtained by the simultaneous solution of light curves and radial velocity data. The orbital period analysis of the system based on $O - C$ data reveals that there exists a periodic variation superimposed on a downward parabola. Although secular changes were noted in previous studies (e.g Çiçek et al. 2005; Siwak et al. 2010), a sinusoidal type variation was discovered in this study. The quadratic term of the parabolic change indicates that the orbital period is decreasing at a rate of $dP/dt = -1.5 \times 10^{-7} \text{ d yr}^{-1}$. Such a secular period variation can be attributed to mass transfer between the components. Under the assumption of conservative mass transfer, the mass transfer rate can be estimated by the following equation (Singh & Chaubey 1986)

$$\frac{\dot{P}}{P} = \frac{3(1-q)}{q} \frac{\dot{M}_1}{M_1}, \quad (5)$$

where M_1 and \dot{M}_1 are the mass of the primary component and its rate of change, respectively. While q indicates the mass ratio for the components, P and \dot{P} are

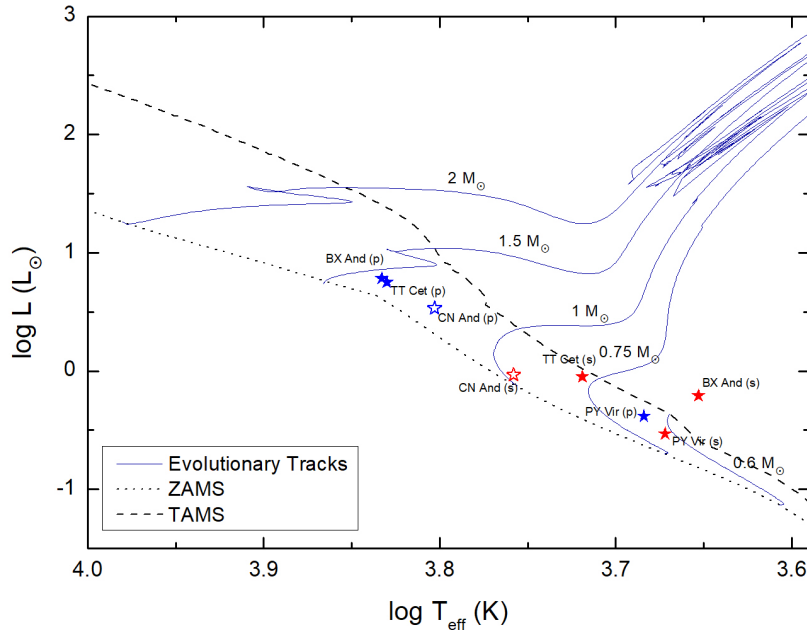


Fig. 6 Positions of primary and secondary components of shallow contact binaries CN And, BX And, TT Cet and PY Vir in the $\log T_{\text{eff}} - \log L$ plane. Evolutionary tracks, and ZAMS and TAMS lines were constructed using solar chemical composition based on MIST single star models.

the orbital period and its decreasing rate for the system, respectively. Based on the parameters obtained from orbital period analysis and the results of light and radial curve analysis, the mass transfer rate from the more massive component to the less massive one can be calculated as $dM_1/dt = -9.9(1) \times 10^{-8} M_{\odot} \text{ yr}^{-1}$. As a result of the decreasing orbital period of close binaries in the early contact phase (and also of near-contact binaries), they will evolve into the state of deeper contact due to shrinking of the Lagrangian surfaces. In Table 7, some near-contact binaries are listed which are very close to their inner Roche lobes, as well as the shallow contact binaries BX And and TT Cet. All systems in the table show decreasing orbital periods and are candidates for becoming close binary stars with a high degree of contact, as is the case for CN And.

In addition to secular change, the orbital period of CN And indicates cyclic variation in the $O - C$ diagram (see Fig. 5), indicated for the first time in this study. Two possible models were used to interpret this cyclic variation: i) the Applegate model based on a possible magnetic cycle of the primary component of the system and ii) LITE due to the third component around the close binary. Magnetic activity of the primary component can cause cyclic period variation since the light curves of the system were distorted, probably due to a dark spot on the primary sur-

face as given our results in Table 2. In addition, a magnetic spot on the surface of the more massive component was also used in previous studies to represent asymmetries in the light curves of the system (e.g. van Hamme et al. 2001, Çiçek et al. 2005, Lee & Lee 2006). Therefore, cyclic variations in the $O - C$ diagram may result from the magnetic activity process. Assuming cyclic variations in the $O - C$ data can result from magnetic activity of the primary component, we have calculated Applegate model parameters (in Table 5). The required angular momentum transfer between inner and outer parts of the primary component during its magnetic cycle can be calculated to be $\Delta J = 1.0 \times 10^{47} \text{ erg s}^{-1}$, while luminosity variation in the modulation period is found to be $\Delta L_{\text{rms}} = 0.007 L_{\odot}$ using the equations given by Applegate (1992). All model parameters are not far from those suggested by Applegate (1992). In order to get more clues about the magnetic cycle behavior, the spot activity should be followed and also data in the high energy band should be obtained.

Another explanation for periodic variation in $O - C$ data is an unseen third component around the close binary system. Therefore, we have applied the LITE to $O - C$ data together with the parabolic term to derive the properties of a possible third-body and its orbit using equations common in many studies (e.g. Soydugan et al. 2003; Yang

et al. 2010). The period of cyclic variation seen in Figure 5 was found to be 38 ± 4 yr, while the semi-amplitude obtained was 0.0043 ± 0.0002 d. The mass of the tertiary companion could be calculated as $m_3 = 0.11 M_{\odot}$, assuming that the hypothetical third component is coplanar with the close binary ($i_3 = 69.7^{\circ}$). If the third component is a main-sequence star, it could be a fully convective red dwarf star and therefore, during the photometric analysis, a third light contribution was not found. The semi-amplitude of the expected radial velocity variation of the system's mass center may be about 0.6 km s^{-1} . This is very small; therefore, high resolution and time-spread spectra are necessary for its confirmation.

CN And is a rarely seen important system at the early stage of its contact phase. Systems such as this can be very informative for studying evolutionary processes where they pass from being near-contact or cool-detached binaries to contact interacting binaries, and also for testing evolutionary models. Therefore, more sensitive photometric data and high resolution spectra are required to understand the nature of the system(s) in greater detail.

Acknowledgements The authors thank the anonymous referee for the substantial suggestions and comments that enabled us to improve the manuscript. This study was supported by the Scientific Research Fund of Çanakkale Onsekiz Mart University, Turkey (Project No. FDK-2018-2458). We thank the Astrophysics Research Centre and Ulupınar Observatory of Çanakkale Onsekiz Mart University for their support and allowing use of their T30 telescope. The current research forms part of the PhD thesis of M.F. Yıldırım. This work has made use of data from the European Space Agency (ESA) mission *Gaia* (<https://www.cosmos.esa.int/gaia>), processed by the *Gaia* Data Processing and Analysis Consortium (DPAC, <https://www.cosmos.esa.int/web/gaia/dpac/consortium>). Funding for the DPAC has been provided by national institutions, in particular the institutions participating in the *Gaia* Multilateral Agreement. This research has made use of the APASS database, located at the AAVSO web site. Funding for APASS has been provided by the Robert Martin Ayers Sciences Fund. This research made use of VIZIER and SIMBAD databases at CDS, Strasbourg, France.

References

- Applegate, J. H. 1992, *ApJ*, 385, 621
- Bozkurt, S., Ibanoglu, C., Gulmen, O., & Gudur, N. 1976, *Information Bulletin on Variable Stars*, 1087
- Çiçek, C., Erdem, A., & Soyduğan, F. 2005, *Astronomische Nachrichten*, 326, 127
- Choi, J., Dotter, A., Conroy, C., et al. 2016, *ApJ*, 823, 102
- Cox, A. N. 2000, *Allen's Astrophysical Quantities* (New York: AIP Press)
- Deb, S., & Singh, H. P. 2011, *MNRAS*, 412, 1787
- Dotter, A. 2016, *ApJS*, 222, 8
- Drilling, J.S., Landolt, A. U., 2000, in *Allen's Astrophysical Quantities*, ed. A. N. Cox (New York: AIP Press), 1
- Duerbeck, H. W., & Rucinski, S. M. 2007, *AJ*, 133, 169
- Eker, Z., Demircan, O., Bilir, S., & Karataş, Y. 2006, *MNRAS*, 373, 1483
- Evren, S., Ibanoglu, C., Tunca, Z., Akan, M. C., & Keskin, V. 1987, *Information Bulletin on Variable Stars*, 3109
- Flannery, B. P. 1976, *ApJ*, 205, 217
- Gaia Collaboration, Brown, A. G. A., Vallenari, A., et al. 2016, *A&A*, 595, A2
- Gaia Collaboration, Brown, A. G. A., Vallenari, A., et al. 2018, *A&A*, 616, A1 (arXiv:1804.09365)
- Hilditch, R. W., Collier Cameron, A., Hill, G., Bell, S. A., & Harries, T. J. 1997, *MNRAS*, 291, 749
- Hoffmeister, C. 1949, *Astronomische Nachrichten*, 278, 24
- Irwin, J. B. 1959, *AJ*, 64, 149
- Kaluzny, J. 1983, *Acta Astronomica*, 33, 345
- Khaliullina, A. I. 2017, *Astronomy Reports*, 61, 859
- Koju, V., & Beaky, M. M. 2015, *Information Bulletin on Variable Stars*, 6127
- Kreiner, J. M., Kim, C.-H., & Nha, I.-S. 2001, *An Atlas of O-C Diagrams of Eclipsing Binary Stars* (Cracow, Poland: Wydawnictwo Naukowe Akademii Pedagogicznej)
- Kwee, K. K., & van Woerden, H. 1956, *Bull. Astron. Inst. Netherlands*, 12, 327
- Lee, C.-U., & Lee, J. W. 2006, *Journal of Korean Astronomical Society*, 39, 25
- Löchel, K., 1960, *M. V. S. Nos.*, 457
- Lucy, L. B. 1967a, *ZAp*, 65, 89
- Lucy, L. B. 1967b, *ZAp*, 65, 89
- Michaels, E. J., Markworth, N. L., & Rafert, J. B. 1984, *Information Bulletin on Variable Stars*, 2474
- Paxton, B., Bildsten, L., Dotter, A., et al. 2011, *ApJS*, 192, 3
- Paxton, B., Cantiello, M., Arras, P., et al. 2013, *ApJS*, 208, 4
- Paxton, B., Marchant, P., Schwab, J., et al. 2015, *ApJS*, 220, 15
- Qian, S. B., Soonthornthum, B., Xiang, F. Y., Zhu, L. Y., & He, J. J. 2004, *Astronomische Nachrichten*, 325, 714
- Robertson, J. A., & Eggleton, P. P. 1977, *MNRAS*, 179, 359
- Ruciński, S. M. 1969, *Acta Astronomica*, 19, 245
- Rucinski, S. M., Lu, W., & Mochnacki, S. W. 2000, *AJ*, 120, 1133
- Samec, R. G., Laird, H., Mutzke, M., & Faulkner, D. R. 1998, *Information Bulletin on Variable Stars*, 4616
- Shaw, J. S., Caillault, J.-P., & Schmitt, J. H. M. M. 1996, *ApJ*, 461, 951
- Singh, M., & Chaubey, U. S. 1986, *Ap&SS*, 124, 389

- Siwak, M., Zola, S., & Koziel-Wierzbowska, D. 2010, *Acta Astronomica*, 60, 305
- Soydugan, F. 2008, *Astronomische Nachrichten*, 329, 587
- Soydugan, F., Demircan, O., Soydugan, E., & İbanoğlu, C. 2003, *AJ*, 126, 393
- Tsesevich, W. 1956, *Astron. Circ. Kazan*, 170, 14
- van Hamme, W. 1993, *AJ*, 106, 2096
- Van Hamme, W., Samec, R. G., Gothard, N. W., et al. 2001, *AJ*, 122, 3436
- van Hamme, W., & Wilson, R. E. 2003, in *Astronomical Society of the Pacific Conference Series*, 298, *GAIA Spectroscopy: Science and Technology*, ed. U. Munari, 323
- Wilson, R. E., & Devinney, E. J. 1971, *ApJ*, 166, 605
- Yakut, K., & Eggleton, P. P. 2005, *ApJ*, 629, 1055
- Yang, Y.-G., Wei, J.-Y., Kreiner, J. M., & Li, H.-L. 2010, *AJ*, 139, 195
- Yang, Y.-L., & Liu, Q.-Y. 1985, *Information Bulletin on Variable Stars*, 2705
- Zhang, L., Pi, Q., Yang, Y., & Li, Z. 2014, *New Astron.*, 27, 81
- Zhu, L., & Qian, S. 2009, in *Astronomical Society of the Pacific Conference Series*, 404, *The Eighth Pacific Rim Conference on Stellar Astrophysics: A Tribute to Kam-Ching Leung*, eds. B. Soonthornthum, S. Komonjinda, K. S. Cheng, & K. C. Leung, 189
- Zhu, L. Y., Qian, S. B., Liu, N. P., Liu, L., & Jiang, L. Q. 2013, *AJ*, 145, 39
- Zola, S., Kreiner, J. M., Zakrzewski, B., et al. 2005, *Acta Astronomica*, 55, 389